

EMISSION CHARACTERISTICS OF AVIATION KEROSENE COMBUSTION IN AERO-ENGINE ANNULAR COMBUSTOR WITH LOW TEMPERATURE PLASMA ASSISTANCE

by

Xingjian LIU^{a,b*}, Liming HE^b, Yi CHEN^b, Jianping LEI^b, and Jun DENG^b

^aThe 94655 Unit of Chinese Peoples's Liberation Army, Wuhu, Anhui Province, China

^bAeronautics and Astronautics Engineering College, Air Force Engineering University,
Xi'an, Shanxi Province, China

Original scientific paper
<https://doi.org/10.2298/TSCI171002138L>

A plasma-assisted combustion test platform for annular combustor was developed to validate the feasibility of using plasma-assisted combustion actuation to reduce emission levels. Combustor outlet temperature and emission levels of O₂, CO₂, H₂, CO, and NO_x were measured by using a thermocouple and a Testo 350-Pro Flue Gas Analyzer, respectively. Combustor combustion efficiency was also calculated. The effects of duty ratio, feedstock air-flow rate, and actuator position on combustion efficiency and emission performance have been analyzed. The results show that the target of CO and NO_x emissions reduction in plasma-assisted combustion could not be fully achieved for kerosene/air mixture with different combustor excessive air coefficients. It is also shown that plasma-assisted combustion with dilution air hole actuation is superior to that of secondary air hole actuation for the combustion of liquid-kerosene fuel. Besides, plasma-assisted combustion effect is more obvious with an increase of duty ratio or feedstock air-flow rate. These results are valuable for the future optimization of kerosene-fueled aero-engine when using plasma-assisted combustion devices to improve emission performance of annular combustor.

Key words: *non-equilibrium plasma, assisted combustion, annular combustor, kerosene, emission*

Introduction

Combustion of hydrogen fuels has been the most important energy source for many years. About 80% of world energy supply is produced by combustion, and it is very much worthwhile studying and optimizing this process, especially in an aero-engine combustor, which uses liquid fuels of high energy density [1]. However, the energy conversion efficiency of existing gas turbine combustor is still low, and spray combustion of aviation kerosene is always a major concern for air transportation in civil aviation due to the strict GHG regulation and air pollution reduction demand. These new regulations and requirements have posed unprecedented challenges for aero-engine combustor researchers to develop new combustion enhancement technology to drastically increase fuel combustion efficiency and reduce emissions.

Plasma, which is the fourth state of matter, has been demonstrated as an efficient tool and promising technology for influencing combustion-related chemistry, sustaining/intensification of combustion, reduce emissions, and improve flame stabilization owing to its

* Corresponding author, e-mail: lxjkgd@163.com

unique capacity in producing reactive species and heat and modifying transport processes [2]. In the last two decades, great progress has been made in exploring the mechanisms of plasma chemistry interactions and energy distribution method in the discharge process.

Non-equilibrium plasma is a type of plasma in which the electronic, vibrational, and rotational temperatures are very different and the electrons have significantly higher plasma temperature than the other gas components. Typical non-equilibrium plasma includes dielectric barrier discharge, gliding arc discharge, glow discharge, microwave discharge, streamer discharge, and corona discharge. Compared to equilibrium plasma, non-equilibrium plasma is more kinetically active, because it can rapidly produce active radicals and excite species through various plasma chemistry reactions, such as electron impact dissociation, excitation, and subsequent energy relaxation [1-4]. Productions of new species accelerate chain branching reactions and broaden the ignition kernel, while the elevated temperatures from the plasma reduce radical quenching caused by recombination and diffusion to the walls.

Many impressive demonstrations of the advantages of plasma-assisted combustion (PAC) using non-equilibrium plasma discharge in emission control have been made. Dielectric barrier discharge, pulsed corona discharge, gliding arc discharge, and microwave discharge were used as plasma-assisted combustion actuation (PACA) method. These studies have shown that PAC has the prominent capacity to reduce NO_x emission. Recently, by using PAC technology, SO_x [5] and unburned hydrocarbons [5, 6] in flue gas as well as soot formation in the exhausted gas of Diesel engines [7-9] have been successfully removed, which further demonstrate the strong capability of plasma emission control.

The PAC technology will have wider applications in the future due to its obvious advantages. Although previous studies of many researchers have successfully validated the feasibility of PAC, it remains unclear how PAC effect is for liquid-kerosene fueled in the annular combustor of aero-engine, especially its emission control effect. Moreover, detailed emission characteristics are not well known. As such, this paper intends to apply PAC technology to aero-engine combustor and investigate emission characteristics of aviation kerosene combustion in aero-engine annular combustor with low temperature plasma assistance. The goals of this paper is to measure combustion efficiency and emission levels of annular combustor with plasma assistance and compare them with normal combustion (NC) results, so as to validate whether the scheme of PAC in annular combustor designed in this paper is feasible or not and study effects of duty ratio, feedstock air-flow rate, and actuator position on emission characteristics. By creating a clear picture of how emission characteristics of annular combustor are affected by PACA, we can determine how to most effectively utilize this promising technology to exert emission control in aero-engine combustion chamber.

Experimental set-up

A PAC test facility of annular combustor was established, as shown in fig. 1, which consisted of air supply system, fuel supply system, combustor test section, control system, and testing system. High-speed air-flow was generated by an air compressor (OGFD-42.8/8B, nominal cubage flow of $42.8 \text{ m}^3/\text{min}$, nominal exhaust pressure of 0.8 MPa), and then the air-flow enters the annular combustor fan-shaped testpiece with two domes, which was directly cut from a real annular combustor of a service aero-engine, as shown in fig. 2(a). An internal taper flowmeter (DYNZ16-8001E12, measurement error of 2.2%) was used to measure the volumetric flow rate of intake air-flow. A 200 liter stainless drum was filled with aviation kerosene (GB6537-2006, RP-3, China), which was connected with steel fittings to a plunger pump (maximum speed of 3565 rpm, maximum operating pressure of 4052 kPa). A gear

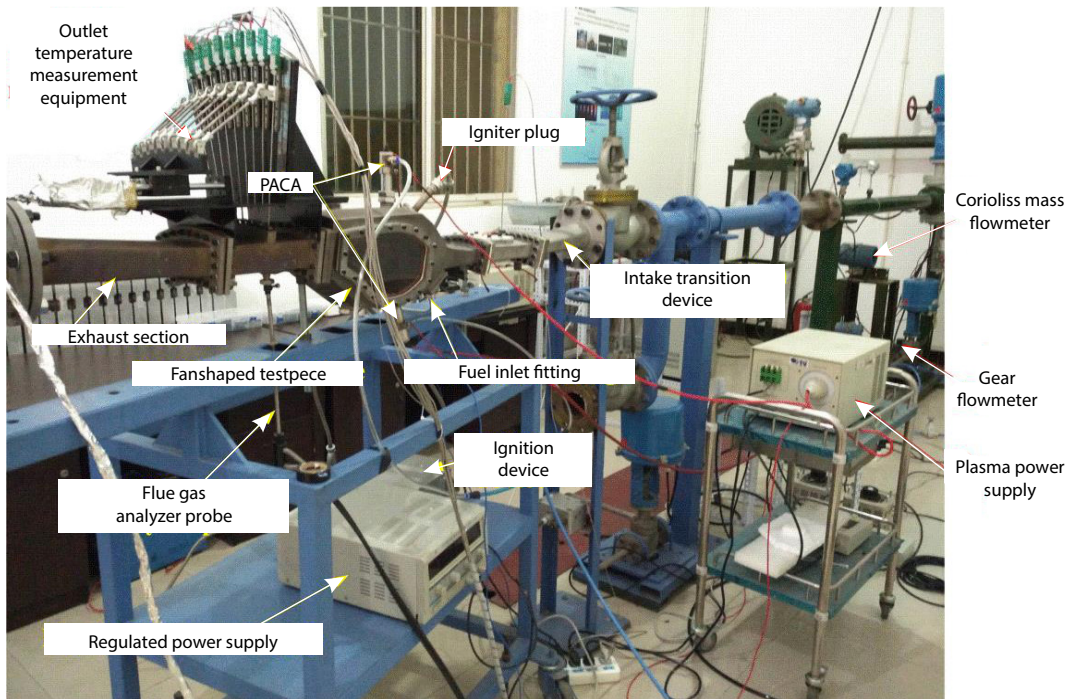


Figure 1. Photograph of PAC test facility of annular combustor

flowmeter (KRACHT, measurement error of 0.3%) was installed to measure the volumetric flow rate of kerosene.

The original fuel spray nozzle and ignition equipment developed by designers of this kind of aero-engine annular combustor were used in this experiment, as shown in figs. 2(b) and 2(c).



Figure 2. Components of PAC test facility; (a) flame tube and annular combustor casing, (b) fuel spray nozzle, and (c) ignition equipment

Figure 3 shows the schematic of PAC test section. The inlet and outlet plane of fanshaped testpiece are both fanlike. The inside and outside diameters of inlet plane are 272.08 mm and 301.8 mm, respectively. The fan angle of inlet plane is 25.71° , therefore, the area of inlet plane is 3351 mm². Besides, a pair of PACA can be mounted to secondary air holes or dilution air holes. Moreover, the thermocouple soleplate, flue gas analyzer probe soleplate, and pressure transducer soleplate were designed in outlet measurement section, which is used for measuring

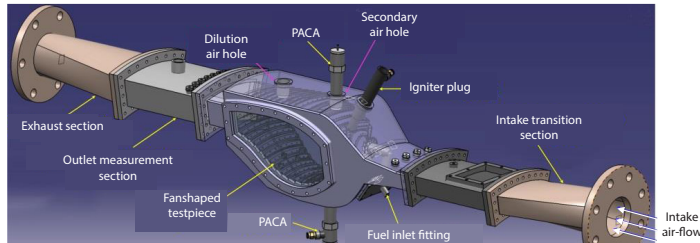


Figure 3. Schematic of PAC test section

outlet temperature, flue gas composition and level, and exhaust gas pressure.

Typical electrode arrangements of cylindrical dielectric barrier discharge are employed to the PACA, as shown in fig. 4, and its characteristics were investigated in our previous work [10]. A pair of PACA was oppositely connected to the fan-shaped testpiece to inject air plasma into combustor. The feedstock air-flow rate of PACA was measured by a mass flowmeter (Sincerity, DMF-1-1-A/DMF-DX, measurement error of $\pm 0.5\%$). The discharge was driven by a sinusoidal plasma power supply (CTP-2000S, Suman Electronics) with a frequency in the range from 5-25 kHz, modulating frequency of 100-1000 Hz, a maximum peak-to-peak voltage of 30 kV, duty ratio of 10-99%, and output power of 500 W.

The outlet temperature measurement equipment was developed to automatically control the motion of thermocouples and log temperature signals of combustor outlet plane, as shown in fig. 5. Nine armored thermocouples (WRNK-1912G, K type, measuring range of 0~1300 °C, reliable accuracy of ± 2.5 °C, thermal response time of

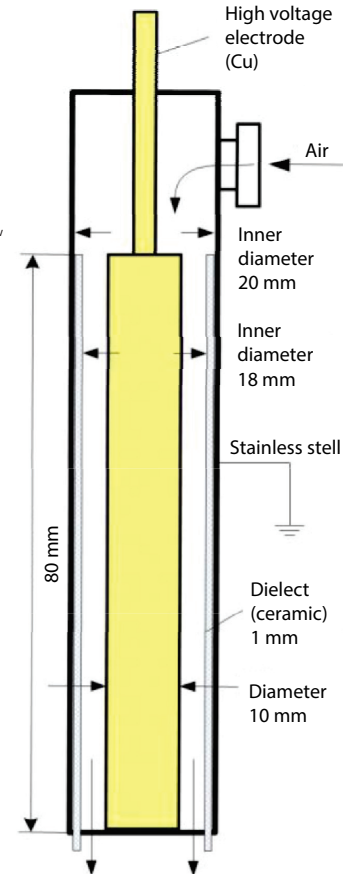


Figure 4. Geometry of PACA

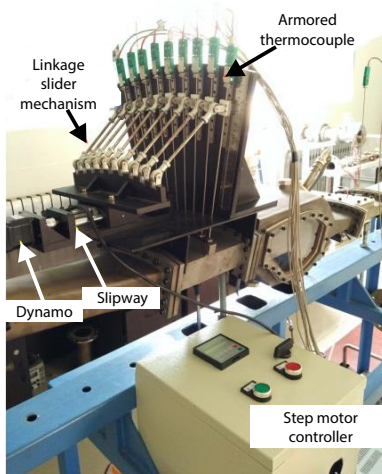


Figure 5. Outlet temperature measurement equipment

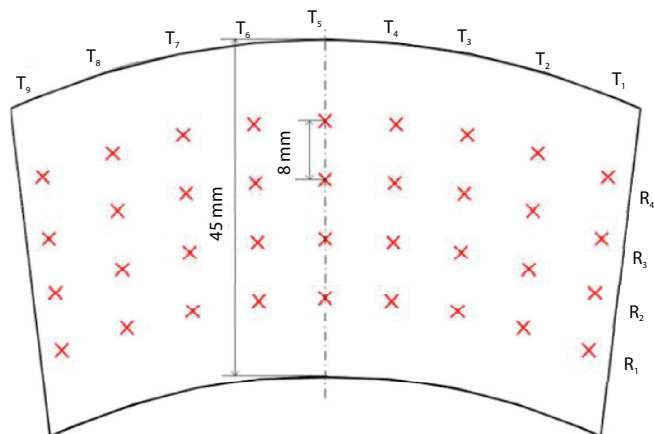


Figure 6. Schematic of outlet temperature measuring point distribution

1.2 second, armored diameter of 3 mm, measurement error of 0.75%) were used to measure temperature signals. The schematic of outlet temperature measuring point distribution is shown in fig. 6. The T₁~T₉ represents the installation position of nine armored thermocouples, and R₁~R₄ stands for fours measuring cambered surfaces. Every cambered surface includes nine temperature measuring points, which are marked as red crosses. Therefore, there is totally 36 outlet temperature measuring points in each test. Besides, an armored thermocouple was installed into intake transition section and used to measure combustor inlet temperature. The signals of these ten armored thermocouples were collected by NI PXIe-1082 and TB-4353, which was manufactured by US National Instruments Corporation.

A Testo 350-Pro Flue Gas Analyzer probe was installed into the exhaust section and its measuring point was arranged in the center of combustor outlet plane to sample heated flue gas. The data from the analyzer was used with Testo EasyEmission software to log data at a one-second interval. The analyzer measures levels of O₂, CO₂, CO, H₂, NO, and NO₂. The technical data of these test models are tabulated in tab. 1. The emission levels of NO_x presented in the following parts of this paper are the sum of NO and NO₂.

Table 1. Technical data of O₂, CO₂, CO, H₂, NO, and NO₂ model of Testo 350-Pro

Probe type	O ₂	CO ₂	CO	H ₂	NO	NO ₂
Range ability	0 ~ +25Vol.%	0 ~ CO ₂ max Vol.% CO ₂	0 ~ +10000 ppm	0 ~ +10000 ppm	0 ~ +3000 ppm	0 ~ +500 ppm
Reliable accuracy	±0.2 Vol.%	Calculated by O ₂	±5% CO ppm	±5% H ₂ ppm	±5 ppm (≤99 ppm); ±5% NO ppm (>99 ppm)	±5 ppm (≤99 ppm); ±5% NO ₂ ppm (>99 ppm)
Resolution ratio	0.01 Vol.%	0.01 Vol.% CO ₂	1 ppm	1 ppm	1 ppm	0.1 ppm
Response time	20 s	20 s	40 s	40 s	30 s	40 s

Results and discussion

In this study, the volumetric flow rate of intake air-flow of the annular combustor fan-shaped testpiece with two domes was set to 180 m³/h, 230 m³/h, and 280 m³/h, respectively. The corresponding inlet velocity magnitude was 14.08 m/s, 17.99 m/s, and 21.90 m/s, respectively. Besides, the volumetric flow rate of fuel was 0.400 L per minute (~0.024 m³/h). Therefore, the combustor excessive air coefficient can be calculated using eq. (1):

$$\alpha = \frac{W_a}{L_0 W_f} \quad (1)$$

where α is combustor excessive air coefficient, W_a – the mass-flow rate of intake air-flow of the annular combustor fan-shaped testpiece with two domes, and W_f – the mass-flow rate of fuel. Besides, W_a and W_f can be calculated from the volumetric flow rates of intake air-flow and fuel using mass-flow rate formula [11]. Moreover, L_0 is theoretical combustion air demand, which denotes the required air-flow mass when the fuel of one kilogram is completely burned. For RP-3 aviation kerosene, $L_0 = 14.7$ kg/kg [12].

The experimental course mainly includes following steps: set-up the assisted-combustion actuation parameters: power supply discharge frequency of 16.26 kHz, modulating frequency of 1000 Hz, duty ratio, applied voltage, and feedstock air-flow rate; switch on the PACA, and collect temperature and flue gas signals simultaneously; fuel spray nozzle works about 3



Figure 7. Ignition run of the annular combustor fan-shaped testpiece

seconds; initiate igniter plug; when the ignition is success and combustion is stable, switch on outlet temperature measurement equipment and log data of outlet temperature; when the flue gas and temperature data are logged over, stop fuel supply and turn off plasma-assisted combustion actuator; cool off the experimental segment for about 30 minutes and then conduct the next test. It is necessary to note that the inlet total pressure is 101.3 kPa in all tests due to the limits of experimental conditions. The ignition run of the annular combustor fan-shaped testpiece is shown in fig. 7.

One of the most important combustor performance parameter is combustion efficiency. It can imply the degree of completeness of fuel combustion. The combustor combustion efficiency is calculated mainly via three different pathways: enthalpy-increase, temperature-rise, and gas composition analysis. Due to the limit of test conditions, the enthalpy-increase combustion efficiency was used in this experimental study. If heat dissipating capacity of the combustor, physical enthalpy difference produced while fuel injecting into the combustor, and heat absorption caused by thermal disassociation of some species are all ignored, the combustor combustion efficiency, η_b , could be obtained by calculating the eq. (2) according to combustor energy equilibrium relation:

$$\eta_b = \frac{\alpha L_0 (i_4^* - i_3^*) + I_4 - I_0}{H_f} \quad (2)$$

where α is combustor excessive air coefficient, L_0 – theoretical combustion air demand, i_3^* and i_4^* – the unit thermal enthalpy of air-flow passed through inlet and outlet plane of combustor, respectively, I_4 – the isothermal combustion enthalpy difference of combustor outlet averaged temperature, and I_0 – the isothermal combustion enthalpy difference of reference temperature. The temperature, 288.15 K, used for measuring lower heating value is served as the reference temperature. The H_f is lower heating value, which value is 42900 kJ/kg for RP-3 aviation kerosene [12]. The values of unit thermal enthalpy and isothermal combustion enthalpy difference under different temperatures can be found from [12]. According to the measurement error of intake air-flow rate, W_a , and fuel-flow rate, W_f , the uncertainties of combustor excessive air coefficient, α , and combustor combustion efficiency, η_b , were both estimated to be 2.29%.

Install a pair of PACA to secondary air holes or dilution air holes, and investigate the effects of duty ratio, feedstock air-flow rate, applied voltage, and actuator position on emission characteristics under different combustor excessive air coefficients.

Normal combustion results

Combustion efficiency and emission levels for normal combustion with secondary or dilution air holes actuation are summarized in the tabs. 2-4. In order to isolate the effect of feedstock air-flow on experimental results and provide a fair comparison platform, feedstock

air-flow was introduced into the PACA for normal combustion as well as PAC. These results can serve as a baseline for later measurements to assess plasma effects.

Table 2. Combustion efficiency and emission levels for normal combustion with secondary air holes actuation ($Q = 40$ g/min)

W_a [m ³ h ⁻¹]	W_f [Lmin ⁻¹]	α	η_b [%]	O ₂ [%]	CO ₂ [%]	CO [ppm]	H ₂ [ppm]	NO _x [ppm]
180	0.400	0.762	25.91	4.67	11.05	1089	413	131
230	0.400	0.974	37.37	2.04	13.18	898	328	14
280	0.400	1.185	50.27	4.03	11.81	565	168	23

Table 3. Combustion efficiency and emission levels for normal combustion with secondary air holes actuation ($Q = 80$ g/min)

W_a [m ³ h ⁻¹]	W_f [Lmin ⁻¹]	α	η_b [%]	O ₂ [%]	CO ₂ [%]	CO [ppm]	H ₂ [ppm]	NO _x [ppm]
180	0.400	0.762	26.22	4.45	11.16	1071	404	125
230	0.400	0.974	37.89	1.98	13.22	876	319	11
280	0.400	1.185	50.90	3.45	12.14	549	158	26

Table 4. Combustion efficiency and emission levels for normal combustion with dilution air holes actuation ($Q = 40$ g/min)

W_a [m ³ h ⁻¹]	W_f [Lmin ⁻¹]	α	η_b [%]	O ₂ [%]	CO ₂ [%]	CO [ppm]	H ₂ [ppm]	NO _x [ppm]
180	0.400	0.762	26.78	4.41	11.23	1062	398	83
230	0.400	0.974	38.51	1.98	13.23	843	307	40
280	0.400	1.185	51.18	3.77	11.98	539	143	22

Effect of duty ratio

The PAC tests with different duty ratios were carried out and compared with normal combustion results. In these tests, the applied voltage was set to 10.1 kV, modulating frequency was set to 1000 Hz, feedstock air-flow rate was set to 40 g/min. These parameters along with a pair of PACA was provided to secondary air holes to eject air plasma into primary combustion zone.

Figure 8 shows the effect of duty ratio on combustion efficiency under different combustor excessive air coefficients. The duty ratio of matched group that normal combustion belongs to amounts to zero in the following figures. As shown in fig. 8, combustion efficiency increases with an increase of combustor excessive air coefficient, which coincides well with typical combustion efficiency characteristics of the annular combustor of a service aero-engine [12]. Since combustor excessive air coefficient was less than the optimum, excessive air coefficient of combustion reduced below the optimal limit. In other words, fuel/air mixing ratio deviates from the most favorable one, which caused combustion efficiency reduction and combustion efficiency decrease. Further, kerosene evaporation and heat absorption capacity increased with increasing kerosene supply quantity, while kerosene/air mixture temperature in combustion zone reduced and a portion of unburned fuel blew away. Therefore, combustion efficiency gradually reduced when combustor excessive air coefficient decreased, as shown in the left half of curves in fig. 9. Because the values of combustor excessive air coefficient in this paper were all less than that of the optimal condition, combustion efficiency increased with an increase of combustor excessive air coefficient.

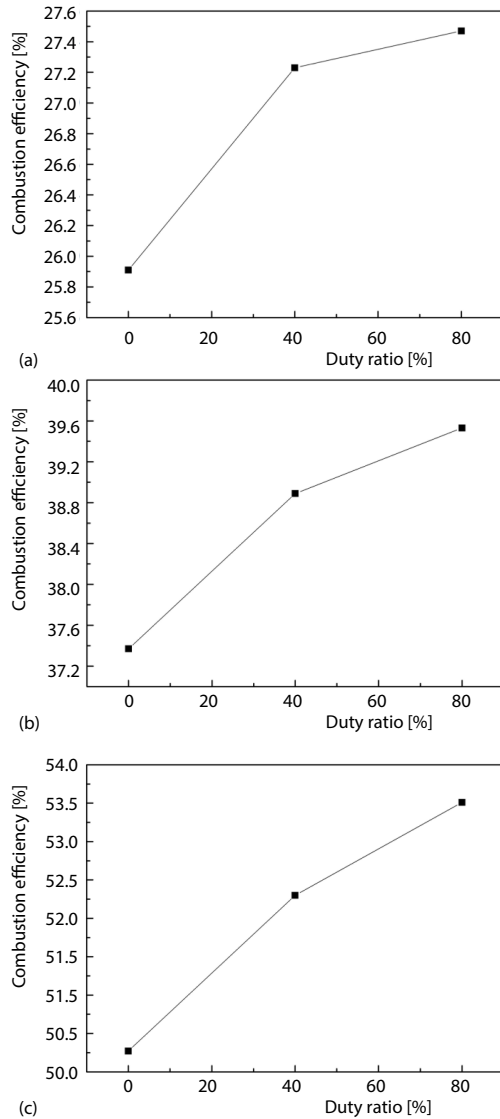


Figure 8. Effect of duty ratio on combustion efficiency with different combustor excessive air coefficients: (a) $\alpha = 0.762$, (b) $\alpha = 0.974$, and (c) $\alpha = 1.185$

mixtures, respectively. Then, the averaged variations of emission levels were obtained by averaging the absolute results of those two groups of the duty ratio. Compared to normal combustion results in the tab. 2, averaged variations of emission levels are: O_2 volume fraction reduced by 0.40%, 0.34%, and 0.65%, respectively; CO_2 volume fraction increased by 0.59%, 0.56%, and 0.60%, respectively; H_2 emission reduced 48 ppm, 61 ppm, and 53 ppm, respectively; CO emission reduced 58 ppm, 116 ppm, and 69 ppm, respectively; NO_x emission from fuel-rich mixture combustion reduced 17 ppm, whereas it increased 37 ppm and 3 ppm, respectively,

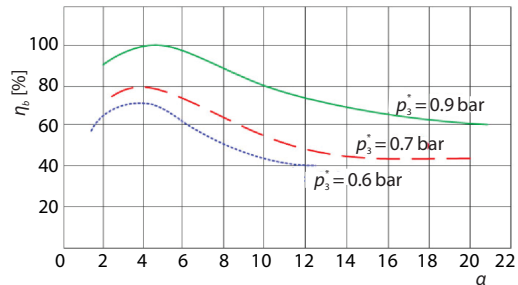


Figure 9. Typical combustion efficiency characteristics of annular combustor of a service aero-engine

For fuel-rich, approximate stoichiometric ratio, and fuel-lean, kerosene/air mixtures, as PACA with different duty ratios was applied, averaged combustion efficiencies of them were 27.35%, 39.21%, and 52.91%, respectively, which increased by 1.44%, 1.84%, and 2.64% when compared to normal combustion results in tab. 2. Figure 8 also suggests that combustion efficiency increases with an increase of duty ratio of plasma power.

Figure 10 shows the effect of duty ratio on emission levels under different combustor excessive air coefficients. For fuel-rich, approximate stoichiometric ratio, and fuel-lean, kerosene/air mixtures with plasma assistance, the tests were made at two values of duty ratio $\beta = 40\%$ and $\beta = 80\%$. Emission levels varied when PACA was applied, and the averaged variations of O_2 , CO_2 , H_2 , CO, and NO_x were investigated in this paper. The absolute variations of emission levels were calculated by comparing PAC test results with those of normal combustion, which was tabulated in tab. 2, at two values of duty ratio $\beta = 40\%$ and $\beta = 80\%$ for fuel-rich, approximate stoichiometric ratio, and fuel-lean, kerosene/air

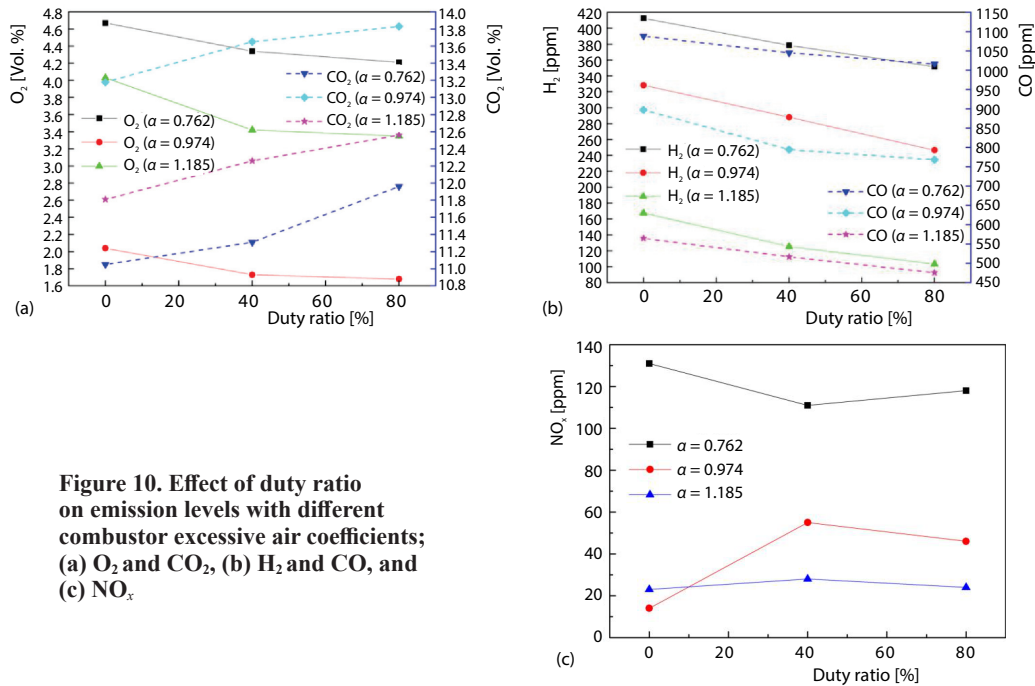


Figure 10. Effect of duty ratio on emission levels with different combustor excessive air coefficients; (a) O_2 and CO_2 , (b) H_2 and CO , and (c) NO_x .

from approximate stoichiometric ratio and fuel-lean mixtures combustion. When PACA was applied, combustion completeness of kerosene/air mixture enhanced and more chemical energy could be converted into thermal energy through kerosene combustion. However, NO_x emissions from approximate stoichiometric ratio and fuel-lean mixtures were higher than that of normal combustion, which does not fully meet our demands. The local higher temperature caused by PAC may be responsible for it. Figure 10 also shows that the variations of averaged emission levels become more significant when duty ratio increased.

Effect of feedstock air-flow rate

Feedstock air-flow is the working gas of PACA, and some kinds of reactive species, such as O_3 , O , $O^2(a^1\Delta_g)$, and $N^2(C^3\Pi_u)$ would be generated by air plasma chemistry reactions. It was found that feedstock air-flow rate had a significant influence on PACA characteristics in our previous work [13], and PAC tests of kerosene/air mixture under different feedstock air-flow rates were carried out in this section. In these tests, the applied voltage was set to 10.1 kV, modulating frequency was set to 1000 Hz, duty ratio was set to 40%, and a pair of PACA was mounted to secondary air holes to inject air plasma into the primary combustion zone.

Figure 11 shows the effect of feedstock air-flow rate on combustion efficiency under different combustor excessive air coefficients. At NC condition, feedstock air-flow was introduced into PACA, but high voltage was not applied. Therefore, plasma discharge did not occur and air plasma was not being injected into combustor for normal combustion. Figure 11 shows that combustion efficiencies for PAC are all greater than normal combustion one under different feedstock air-flow rates. For fuel-rich, approximate stoichiometric ratio, and fuel-lean, kerosene/air mixtures, combustion efficiency increases were different when feedstock air-flow rate changed. When the feedstock air-flow rate was 40 g/min, the increase in combustion efficiency

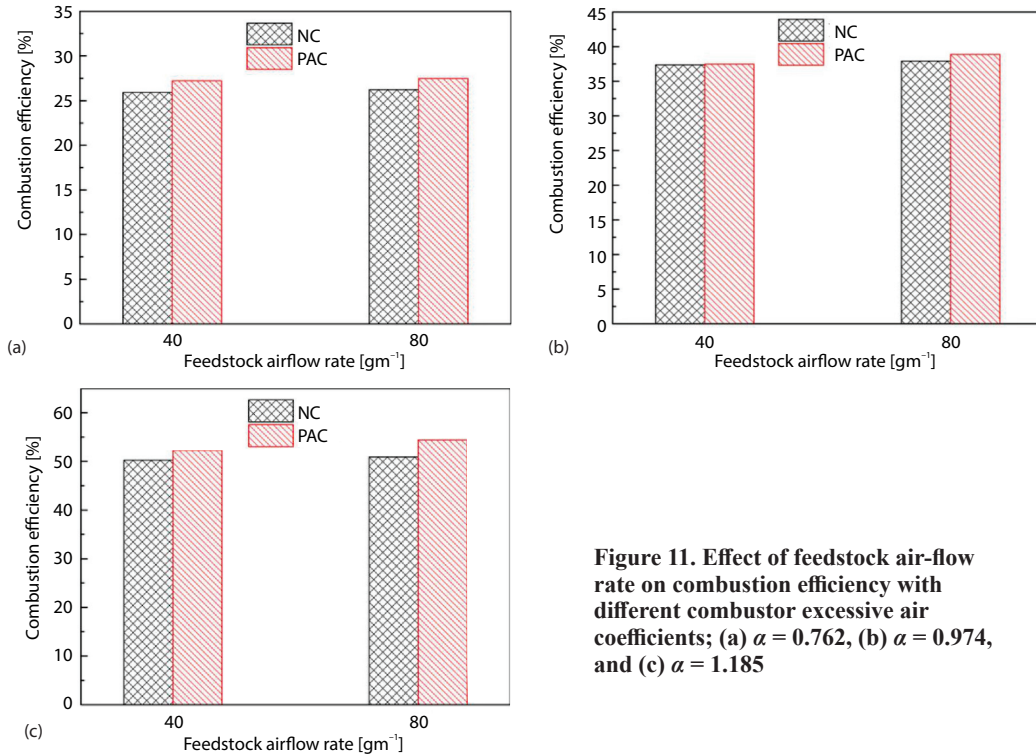


Figure 11. Effect of feedstock air-flow rate on combustion efficiency with different combustor excessive air coefficients; (a) $\alpha = 0.762$, (b) $\alpha = 0.974$, and (c) $\alpha = 1.185$

increase was 1.32%, 0.10%, and 2.03%, respectively. When the feedstock air-flow rate was 80 g/min, combustion efficiency increased by 1.25%, 1.00%, and 3.52%, respectively. In other words, combustion efficiency increased of fuel-lean mixture was the most obvious among all three when the feedstock air-flow rate increased.

Figure 12 shows the effect of feedstock air-flow rate on emission levels under different combustor excessive air coefficients. The absolute variations of emission levels caused by PAC effect for targeted five species were calculated by comparing PAC test results with those of normal combustion, which was tabulated in tabs. 2 and 3 at a volumetric feedstock air-flow rate of $Q = 40 \text{ g/min}$ and $Q = 80 \text{ g/min}$ for fuel-rich, approximate stoichiometric ratio, and fuel-lean, kerosene/air mixtures, respectively. Note, the comparison was only made between PAC and normal combustion with the identical feedstock air-flow rate. Then, the averaged variations of emission levels were obtained by averaging the absolute results of those two groups of volumetric feedstock air-flow rate. The averaged variations of emission levels are: O_2 volume fraction reduced by 0.30%, 0.21%, and 0.40%, respectively; CO_2 volume fraction increased by 0.54%, 0.54%, and 0.53%, respectively; H_2 emission reduced 47 ppm, 58 ppm, and 47 ppm, respectively; CO emission reduced 48 ppm, 109 ppm, and 69 ppm, respectively. Besides, only when PACA was applied to the fuel-rich mixture, NO_x emission from PAC decreased, whereas it increased for approximate stoichiometric ratio and fuel-lean kerosene/air mixtures. Figure 12 also illustrates that when the feedstock air-flow rate increased from 40 g/min to 80 g/min, O_2 volume fraction, H_2 and CO emissions decreased, while CO_2 volume fraction increased, and NO_x emissions from fuel-rich and approximate stoichiometric ratio mixtures combustion decreased, while it increased for fuel-lean mixture combustion.

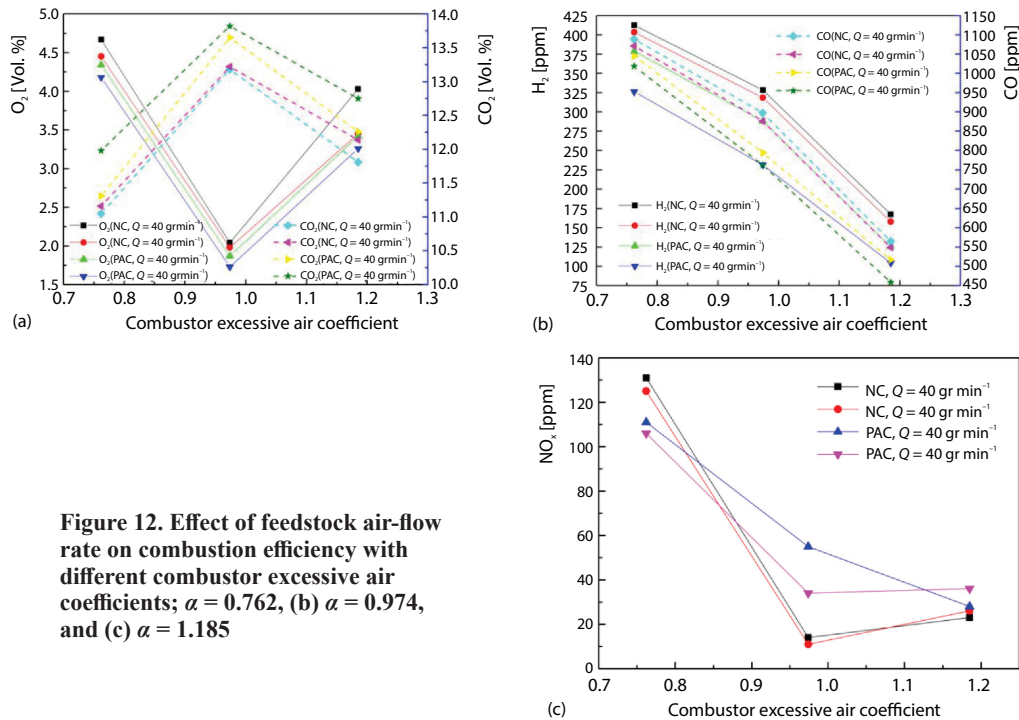


Figure 12. Effect of feedstock air-flow rate on combustion efficiency with different combustor excessive air coefficients; (a) $\alpha = 0.762$, (b) $\alpha = 0.974$, and (c) $\alpha = 1.185$

Effect of actuator position

As aforementioned design scheme, PACA can be connected either to the secondary air holes or to the dilution air holes. Actuator position is considered as an important factor affecting combustor performance with plasma assistance [14]. The PAC tests with different actuator positions were carried out and compared to normal combustion results. In these tests, applied voltage was set to 10.1 kV, modulating frequency was set to 1000 Hz, feedstock air-flow rate was set to 40 g/min, and a pair of PACA was mounted to the dilution air holes to inject air plasma into dilution zone.

Figure 13 shows the effect of actuator position on combustion efficiency under different combustor excessive air coefficients. Several results can be obtained from fig. 13. Firstly, combustion efficiencies of normal combustion under different combustor excessive air coefficients increased when PACA were moved from secondary air holes to dilution air holes. Atomizing liquid kerosene in primary combustion zone could not be completely burned and a portion of unburned fuel would enter mixing region. Second combustion reaction occurring in mixing region was intensified when fresh air was introduced into combustor through dilution air holes, which led to the combustion efficiency enhancement.

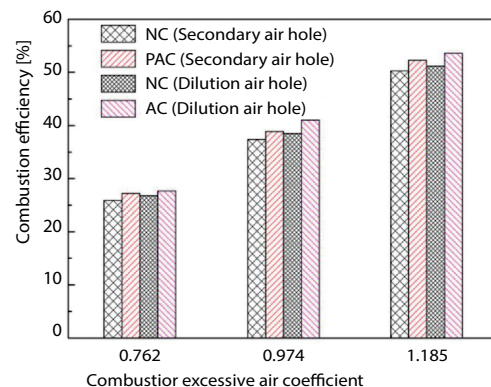


Figure 13. Effect of actuator position on combustion efficiency with different combustor excessive air coefficients

Secondly, for a specified combustor excessive air coefficient, whether PACA were mounted to secondary air holes or dilution air holes, combustion efficiency of PAC was larger than that of normal combustion.

Thirdly, combustion efficiencies with plasma assistance at dilution air holes were larger than those of secondary air holes for any combustor excessive air coefficient.

Figure 14 shows the effect of actuator position on emission levels under different combustor excessive air coefficients. As shown in fig. 14, for fuel-rich, approximate stoichiometric ratio, and fuel-lean, kerosene/air mixtures without plasma assistance, when the feedstock air-flow introduction pathway moved from secondary air holes to dilution air holes, emission levels of O_2 , CO_2 , H_2 , CO , and NO_x change. The major change includes a reduction in O_2 volume fraction, an increase in CO_2 volume fraction, and a reduction in CO and H_2 emissions reduced. Besides, NO_x emissions from the fuel-rich mixture combustion reduced, and it is seen to increase for approximate stoichiometric ratio mixture. However, it changed slightly for fuel-lean mixture. It was also found that CO and H_2 emissions reduced when PACA was applied to annular combustor whether through secondary air holes or dilution air holes. However, NO_x emissions from approximate stoichiometric ratio and fuel-lean kerosene/air mixture combustion with plasma assistance increased. Finally, comparing emission test results of PAC under different actuator positions, it was found that when PACA were mounted onto the dilution air holes, H_2 and CO emissions lowered and NO_x emission increment reduced. It illustrates that PAC with dilution air holes actuation is superior to that of secondary air holes actuation for the combustion of liquid-kerosene fuel.

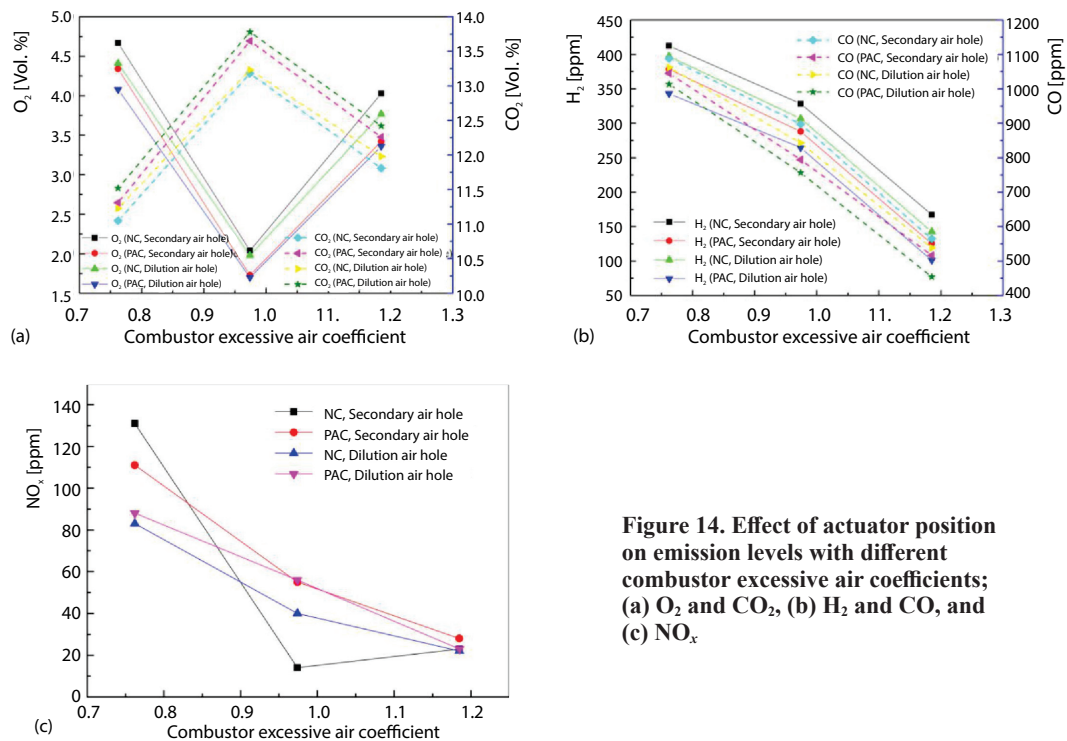


Figure 14. Effect of actuator position on emission levels with different combustor excessive air coefficients; (a) O_2 and CO_2 , (b) H_2 and CO , and (c) NO_x .

Conclusions

By using a pair of PACA with volume dielectric barrier discharge configuration, successful liquid aviation kerosene fueled combustion experiment was carried out in a well-defined aero-engine annular combustor fanshaped testpiece with two domes. The investigations were conducted by temperature and emission measurements. Effects of duty ratio, feedstock air-flow rate, and actuator position on emission characteristics under different combustor excessive air coefficients were presented. Compared to the normal combustion results, the conclusion has been drawn as following.

- When air plasma was injected into the annular combustor, combustion efficiency increased and CO emission reduced for fuel-rich, approximate stoichiometric ratio, and fuel-lean, kerosene/air mixtures. However, NO_x emission reduction was observed only for fuel-rich mixture. The target of CO and NO_x emissions reduction in PAC was not fully achieved.
- Combustion efficiency and CO emission decreased with the increase of duty ratio or feedstock air-flow rate and the NO_x emission's varied for fuel-rich, approximate stoichiometric ratio, and fuel-lean, kerosene/air mixtures.
- Due to occurrence of second combustion when the feedstock air-flow of PACA was introduced into dilution region, PAC effect was more obvious with dilution air holes actuation, which was better for the organization of combustion in annular combustor.
- Applying plasma actuation for the combustion of liquid kerosene fuel in an aero engine could increase combustion efficiency and emission performance. However, the effect is marginal. The obvious drawback is that emission levels of NO_x for approximate stoichiometric ratio and fuel-lean kerosene/air mixture become larger when non-equilibrium plasma actuation was applied. Deeper mechanisms remain to be studied further. The advantage and drawback should be balanced for application in real aero-engine.

For this experiment, it still can be improved a lot. Firstly, it is necessary to increase experimental combustor excessive air coefficient, larger than the optimal one, to obtain its combustor performance parameters, and make a comparison with the test results of this paper. Secondly, the lean blowout characteristic need to be measured, which is another important combustor performance parameter. Finally, total pressure and temperature of combustor intake air-flow should approach to real high altitude environment of aero-engine, and it will be more valuable.

Acknowledgment

This paper could not appear without the help and support of many people who care about plasma-assisted combustion technology. First and foremost, we would like to acknowledge the support of 5719 Factory, who provided us with an annular combustor of a service aero-engine for our research work. Besides, the support of the Key Program of National Natural Science Foundation of China (NNSFC) under Grant Nos. 51436008 was especially important for our team.

Nomenclature

H_f	– lower heating value, [Jkg ⁻¹]	I_0	– isothermal combustion enthalpy difference of reference temperature, [Jkg ⁻¹]
i_3^*	– unit thermal enthalpy of air-flow passed through combustor inlet plane of combustor, [Jkg ⁻¹]	I_4	– isothermal combustion enthalpy difference of combustor outlet averaged temperature, [Jkg ⁻¹]
i_4^*	– unit thermal enthalpy of air-flow passed through combustor outlet plane of combustor, [Jkg ⁻¹]	L_0	– theoretical combustion air demand, [kgkg ⁻¹]
		Q	– volumetric flow rate of feedstock air-flow, [Lmin ⁻¹]

U – applied voltage of plasma-assisted combustion actuator, [kV]
 W_a – mass-flow rate of combustor intake air-flow, [kgs⁻¹]
 W_f – mass-flow rate of fuel, [kgs⁻¹]

Greek symbols

α – combustor excessive air coefficient
 β – duty ratio of plasma power
 η_b – combustor combustion efficiency, [%]

References

- [1] Ju, Y., Sun, W. T., Plasma Assisted Combustion: Dynamics and Chemistry, 2015, *Progress in Energy and Combustion Science*, 48 (2015), 2, pp. 21-83
- [2] Starikovskaia, S. M., Plasma-Assisted Ignition and Combustion: Nanosecond Discharges and Development of Kinetic Mechanisms, *Journal of Physics D: Applied Physics*, 47 (2014), 35, 353001
- [3] Hicks, A., et al., Singlet Oxygen Generation in a High Pressure Non-Self-Sustained Electric Discharge, *Journal of Physics D: Applied Physics*, 38 (2005), 20, pp. 3812-3824
- [4] Brethes-Dupouey, S., et al., 2000, Removal of H₂S in Air by Using Gliding Discharges, *European Physics Journal of Applied Physics*, 11 (2000), 1, pp. 43-58
- [5] Du, C. M., et al., Decomposition of Toluene in a Gliding Arc Discharge Plasma Reactor, *Plasma Sources Science and Technology*, 16 (2007), 4, pp. 791-797
- [6] Yu, L., et al., Destruction of Acenaphthene, Fluorene, Anthracene and Pyrene by a DC Gliding Arc Plasma Reactor, *Journal of Hazardous Materials*, 180 (2010), 1, pp. 449-455
- [7] Fureby, C., et al., Investigation of Microwave Stimulation of Turbulent Flames with Implications to Gas Turbine Combustor, *Proceedings*, 55th AIAA Aerospace Science Meeting, 9-13 January, Grapevine, Tex., USA, AIAA pp. 2017-1779
- [8] Kim, G. T., et al., Effects of Applying Non-Thermal Plasma on Combustion Stability and Emission of NO_x and CO in a Model Gas Turbine Combustor, *Fuel*, 194 (2017), 1, pp. 321-328
- [9] De Giorgi, M. G., et al., Improvement of Lean Flames Stability of Inverse Methane/Air Diffusion Flame by Using Coaxial Dielectric Plasma Discharge Actuators, *Energy*, 126 (2017), 3, pp. 689-706
- [10] Liu, X. J., et al., Experimental Investigation of Effects of Airflows on Plasma-Assisted Combustion Actuator Characteristics, *Chinese Physics B*, 24 (2015), 4, pp. 045101
- [11] Chen, T. N., *Applied Fluid Mechanics*, Aviation Industry Press, Beijing, China, 2006
- [12] He, L. M., *Principles of Aircraft Propulsion System*, National Defense Industry Press, Beijing, China, 2006
- [13] Liu, X. J., et al., Experimental Investigation of Effects of Airflows on Plasma-Assisted Combustion Actuator Characteristics, *Chinese Physics B*, 24 (2015), 4, 045101
- [14] Xiao, H. L., et al., An Experimental Study of the Combustion and Emission Performance of 2,5-Dimethylfuran Diesel Blends on a Diesel Engine, *Thermal Science*, 21 (2017), 1, pp. 543-553